A nonlinear constitutive relationship for the v^2-f model

By B. A. Pettersson Reif

1. Motivation and objectives

Boussinesq's linear eddy-viscosity hypothesis constitutes the foundation of turbulence closures used in industrial CFD computations. This simple stress-strain relationship is particularly attractive since it is easily implemented into general purpose Navier-Stokes solvers in addition to promote numerical stability. These are the primary reasons for its popularity among CFD code developers. However, assumptions inherent in this simple constitutive relationship limits the applicability in many practical applications. Among them is their frame indifferent property.

Pettersson Reif *et al.* (1999) developed a new method to incorporate effects of inertial forces arising from e.g. an imposed rotation of the reference frame into linear eddy-viscosity closures; a modified $v^2 - f$ model was subsequently proposed. A major shortcoming of traditional eddy-viscosity closures could thus be removed, including the original $v^2 - f$ model (Durbin 1991).

The present study focuses on another inherent shortcoming; the equipartitioning of turbulent kinetic energy among the diagonal components of the Reynolds stress tensor in parallel shear flows. The objective is to develop an internally consistent nonlinear $v^2 - f$ model. In other words, the wall-normal Reynolds stress component in parallel shear flow in an inertial frame of reference should equate the scalar v^2 in the new model. The novelty of the new model is that the elliptic relaxation approach then can be used in conjunction with a nonlinear constitutive relationship. The present study is in part motivated by earlier work of Durbin (1995). The premise of the work is that the predictive capability of the $v^2 - f$ could be further increased by accounting for turbulence anisotropy in turbulent shear flows. This requires a nonlinear constitutive relationship.

2. Accomplishments

Following Pope (1975), the equilibrium solution of a second-moment closure (SMC) for a two-dimensional mean flow of an incompressible fluid in a noninertial frame of reference can be expressed as

$$\frac{\overline{\mathrm{uu}}}{k} = \frac{2}{3}\mathrm{I} - a_1\tau_1\mathrm{S} - a_2\tau^2\left[\mathrm{SW}^* - \mathrm{W}^*\mathrm{S}\right] + a_3\tau^2\left[\mathrm{S}^2 - \frac{1}{3}|S^2|\mathrm{I}\right] \tag{1}$$

where

$$S_{ij} = \frac{1}{2}\left(\frac{\partial U_i}{\partial x_j} + \frac{\partial U_j}{\partial x_i}\right), W_{ij}^* = \frac{1}{2}\left(\frac{\partial U_i}{\partial x_j} - \frac{\partial U_j}{\partial x_i}\right) - C_\omega \epsilon_{jik}\Omega_k \tag{2}$$

are the mean rate of strain and normalized mean intrinsic vorticity tensors, respectively. The coefficients a_i in (1) are in general functions of the invariants

$|S^2| = S_{lk}S_{kl}$ and $|W^2| = -W^*_{lk}W^*_{kl}$ as well as turbulent scalar quantities. τ is a turbulent time scale and I is the identity matrix. The coefficient C_ω in (2b) depends on the model for the pressure-strain correlation.

Based on (1), the following constitutive relation for the $\overline{v^2} - f$ model is proposed;

$$\frac{\overline{\mathrm{uu}}}{k} = \frac{2}{3}\mathrm{I} - C^*_{\mu 1}\frac{\overline{v^2}}{k}\tau_1 \mathrm{S} - C^*_{\mu 2}V_1\tau^2\left[\mathrm{SW}^* - \mathrm{W}^*\mathrm{S}\right] + C^*_{\mu 3}V_2\tau^2\left[\mathrm{S}^2 - \frac{1}{3}|S^2|\mathrm{I}\right] \quad (3)$$

where V_i and $C^*_{\mu i}$ can be functions of $\overline{v^2}/k$ and the dimensionless velocity-gradient parameters

$$\eta_1 \equiv \tau^2 S_{ik}S_{ik}\eta_2 \equiv \tau^2 W^*_{ik}W^*_{ik}. \quad (4)$$

The realizability constraint together with the principle of internal consistency will be used in the following subsections to derive the basic form of the new model.

2.1 Realizability

Realizability constitutes a basic physical and mathematical principle which any closure model should obey. Although its practical importance may not be of crucial importance, it nevertheless offers a useful mathematical tool in model development. In terms of the individual components of the Reynolds stress tensor, the realizability constraints can be summarized as:

(i) $\overline{u^2_\alpha} \geq 0$

(ii) $\overline{u^2_\alpha} \leq 2k$

(iii) $(\overline{u_\alpha u_\beta})^2 \leq \overline{u^2_\alpha}\,\overline{u^2_\beta}$

For a general 2D incompressible flow, the mean rate of strain and vorticity tensors can be written as

$$\mathrm{S} = \begin{pmatrix} \lambda & 0 & 0 \\ 0 & -\lambda & 0 \\ 0 & 0 & 0 \end{pmatrix} \quad (5)$$

$$\mathrm{W}^* = \begin{pmatrix} 0 & \omega & 0 \\ -\omega & 0 & 0 \\ 0 & 0 & 0 \end{pmatrix} \quad (6)$$

in principal axes of S. Then $|S^2| = 2\lambda^2$ and $|W^2| = 2\omega^2$ such that $\eta_1 = 2\tau^2\lambda^2$ and $\eta_2 = 2\tau^2\omega^2$. The individual nonzero components of the Reynolds stress tensor (3) are then given by

$$\frac{\overline{u_1^2}}{k} = \frac{2}{3} - 2C^*_{\mu 1}\frac{v^2}{k}\tau_1\lambda + \frac{1}{3}C^*_{\mu 3}V_2\tau^2\lambda^2 \quad (7)$$

$$\frac{\overline{u_2^2}}{k} = \frac{2}{3} + 2C^*_{\mu 1}\frac{v^2}{k}\tau_1\lambda + \frac{1}{3}C^*_{\mu 3}V_2\tau^2\lambda^2 \quad (8)$$

$$\frac{\overline{u_3^2}}{k} = \frac{2}{3} - \frac{2}{3} C^*_{\mu 3} V_2 \tau^2 \lambda^2 \tag{9}$$

$$\frac{\overline{u_1 u_2}}{k} = -2 C^*_{\mu 2} V_1 \tau^2 (\omega \lambda) \tag{10}$$

It then follows from realizability constraint (i) and (9) that

$$C^*_{\mu 3} \leq \frac{1}{V_2 \tau^2 \lambda^2} = \frac{1}{V_2 \frac{1}{2} \eta_1}, \tag{11}$$

from (ii) and (8)

$$C^*_{\mu 3} \leq \frac{\frac{4}{3} - 2 C^*_{\mu 1} \frac{\overline{v^2}}{k} \tau_1 \lambda}{\frac{1}{3} V_2 \tau^2 \lambda^2} = \frac{\frac{4}{3} - C^*_{\mu 1} \frac{\overline{v^2}}{k} \sqrt{2 \eta_1}}{\frac{1}{6} V_2 \eta_1} \tag{12}$$

and finally from (iii) and (7), (8), and (10)

$$C^{*2}_{\mu 2} \leq \frac{\frac{4}{9} \left(1 + C^*_{\mu 3} V_2 \tau^2 \lambda^2 + \frac{1}{4} \left(C^*_{\mu 3} V_2 \tau^2 \lambda^2\right)^2\right) - \left(2 C^*_{\mu 1} \frac{\overline{v^2}}{k} \tau_1 \lambda\right)^2}{4 V_1^2 \tau^4 \omega^2 \lambda^2} \tag{13}$$

Let us now assume that $C^*_{\mu i} \geq 0$. Then, (11) – (13) constitutes useful constraints to arrive at a physically realistic model. In order to retain the previous success of the original model in parallel shear flow, we want to keep the previously used coefficient $C^*_{\mu 1}$ (Durbin 1991 or Pettersson Reif *et al.* 1999). The present study adopts an upper bound on the timescale τ_1 as proposed by Durbin (1995), i.e.

$$\tau_1 \leq \frac{2k}{3 C^*_{\mu 1} \overline{v^2}} \frac{1}{\sqrt{\xi |S^2|}}. \tag{14}$$

where $\xi = 2$ in 2D flow. This constraint on τ_1 ensures that $C^*_{\mu 2}$ and $C^*_{\mu 3}$ are positive, cf. (12) and (13), and it also implies that (11) becomes a more stringent constraint on $C^*_{\mu 3}$ than (12).

Equation (13) can be written as

$$C^*_{\mu 2} \leq \frac{A}{2 V_1 \tau^2 \sqrt{\omega^2 \lambda^2}} = \frac{A}{V_1 \sqrt{\eta_1 \eta_2}} \tag{15}$$

where

$$A = \sqrt{\frac{4}{9} \left(1 + \alpha_0 + \frac{1}{4} \alpha_0^2\right)^2 - \left(2 C^*_{\mu 1} \frac{\overline{v^2}}{k} \tau_1 \lambda\right)^2} \tag{16}$$

if (11) is written on the form $C^*_{\mu 3} V_2 \tau^2 \lambda^2 = \alpha_0$ (where $\alpha_0 \leq 1$). Equations (11) and (15) will be used as templates for the coefficients $C^*_{\mu 3}$ and $C^*_{\mu 2}$, respectively.

Let us choose the following forms

$$C^*_{\mu 2} = \frac{\beta_0 A}{\beta_1 + V_{10}\sqrt{\eta_1\eta_2}} \tag{17}$$

and

$$C^*_{\mu 3} = \frac{\gamma_0}{\gamma_1 + V_{20}\eta_1} \tag{18}$$

where $V_{10} \geq V_1$, $V_{20} \geq \frac{1}{2}V_2$, $\beta_0 \leq 1$, $\gamma_0 \leq 1$, $\beta_1 \geq 0$ and $\gamma_1 \geq 0$ must be imposed in order to satisfy the inequalities (11) and (15). For simplicity, let us choose $\beta_0 = \gamma_0 = 1$. Recall that $\alpha_0 \leq 1$.

The coefficients β_1 and γ_1 are only introduced with the objective to avoid singularities. It is therefore desirable that $\beta_1 << 1$ and $\gamma_1 << 1$ if $\eta_1 >> 1$ and $\sqrt{\eta_1\eta_2} >> 1$, respectively. Also, when $\eta_1, \eta_2 \to 0$, $C^*_{\mu 3}, C^*_{\mu 3} << 1$. This can readily be obtained by choosing the following simple functional forms

$$\beta_1 \propto (0.1 + \sqrt{\eta_1\eta_2})^{-1} \, \gamma_1 \propto (0.1 + \eta_1)^{-1} \tag{19}$$

In order to determine the remaining model parameters, an additional constraint will be used in the next section, namely that the nonlinear constitutive relation should reduce to $\overline{u_2^2} \approx \overline{v^2}$ in parallel shear flow in an inertial frame of reference. Here $\overline{u_2^2}$ denotes the wall-normal component of the Reynolds stress tensor in parallel shear flow.

2.2 Internal consistency

Consider parallel shear flow where $S_{12} = S_{21} = W^*_{12} = -W^*_{21}$ so that $\tau S_{12} = \sqrt{\eta_1/2}$. Assume furthermore that $\eta_1 >> 1$ (which is a valid assumption in the vicinity of a solid boundary; $\eta_1 \approx 60$ in the loglayer). The diagonal elements of (3) can then be written as

$$\frac{\overline{u_1^2}}{k} = \frac{2}{3} + C^*_{\mu 2}V_1\eta_1 + \frac{1}{6}C^*_{\mu 3}V_2\eta_1 \tag{20}$$

$$\frac{\overline{u_2^2}}{k} = \frac{2}{3} - C^*_{\mu 2}V_1\eta_1 + \frac{1}{6}C^*_{\mu 3}V_2\eta_1 \tag{21}$$

$$\frac{\overline{u_3^2}}{k} = \frac{2}{3} - \frac{1}{3}C^*_{\mu 3}V_2\eta_1 \tag{22}$$

where

$$C^*_{\mu 2} \approx \frac{A}{V_{10}\eta_1}, C^*_{\mu 3} \approx \frac{1}{V_{20}\eta_1} \tag{23}$$

Note: since $\eta_1 = \eta_2 >> 1$ the coefficients β_1 and γ_1 in (17) and (18) can be neglected. Internal consistency then requires that

$$\frac{\overline{u_2^2}}{k} = \frac{\overline{v^2}}{k}(21) \Rightarrow \frac{2}{3} - \beta_0 A\frac{V_1}{V_{10}} + \frac{1}{6}\gamma_0\frac{V_2}{V_{20}} = \frac{\overline{v^2}}{k} \tag{24}$$

Given the following parameters (in the limit $\eta_1 >> 1$)

$$\frac{V_1}{V_{10}} = \frac{V_2}{V_{20}} = \frac{6}{5}\left(\frac{2}{3} - \frac{\overline{v^2}}{k}\right) \tag{25}$$

(24) can be written as

$$\frac{2}{3} + \frac{6}{5}\left(\frac{1}{6} - A\right)\left(\frac{2}{3} - \frac{\overline{v^2}}{k}\right) = \frac{\overline{v^2}}{k} \Rightarrow A = 1. \tag{26}$$

However, since A varies according to (16), the internal consistency constraint can only be approximately fulfilled. With $\alpha_0 = 1$, (16) becomes

$$A = \sqrt{1 - \left(2C^*_{\mu 1}\frac{\overline{v^2}}{k}\right)^2 \frac{1}{2}\eta_1} \tag{27}$$

which in is parallel shear flow is equivalent to

$$A = \sqrt{1 - \left(\frac{\overline{uv}}{k}\right)^2} \approx 1 \tag{28}$$

Recall that $\overline{uv}/k \approx 0.30$ in the loglayer. The present nonlinear constitutive relationship for the $\overline{v^2} - f$ model thus satisfies realizability in 2D as well as being internally consistent in the two-component limit; $A \to 1$ as $y \to 0$.

2.3 Assessment of the new model

The final form of the model is given by

$$\overline{u_i u_j} = \frac{2}{3}k\delta_{ij} - 2C^*_{\mu 1}\overline{v^2}\tau_1 S_{ij} - Vk\tau^2\left[C^*_{\mu 2}\left(S_{ik}W^*_{kj} + S_{jk}W^*_{ki}\right) - C^*_{\mu 3}\left(S_{ik}S_{kj} - \frac{1}{3}|S^2|\delta_{ij}\right)\right] \tag{29}$$

where

$$C^*_{\mu 1} = C_\mu F \tag{30}$$

$$C^*_{\mu 2} = \frac{6}{5}\frac{\sqrt{1 - \left(C^*_{\mu 1}\frac{\overline{v^2}}{k}\right)^2 2\eta_1}}{\beta_1 + \sqrt{\eta_1\eta_2}} \tag{31}$$

$$C^*_{\mu 3} = \frac{6/5}{\gamma_1 + \eta_1} \tag{32}$$

and

$$V = max\left[\frac{2}{3} - \frac{\overline{v^2}}{k}, 0\right], \beta_1 = \frac{1}{0.1 + \sqrt{\eta_1\eta_2}}, \gamma_1 = \frac{1}{0.1 + \eta_1} \tag{33}$$

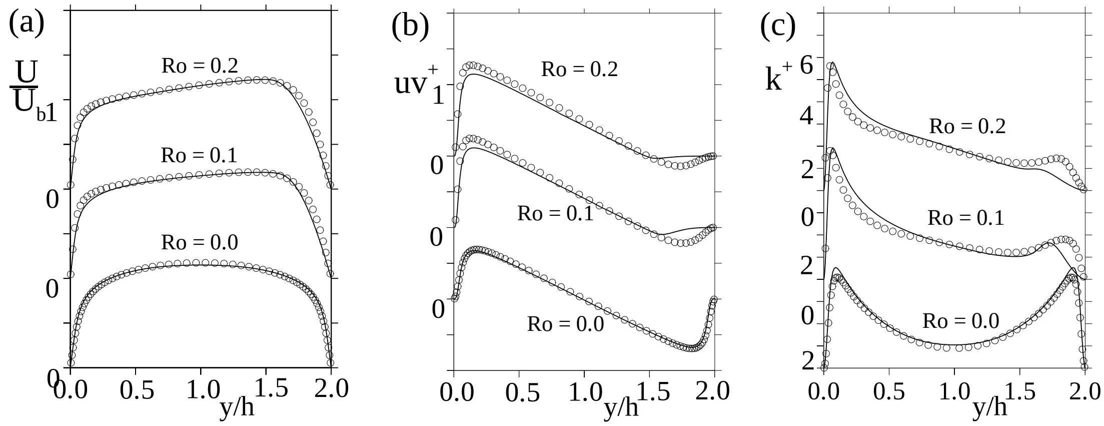

FIGURE 1. Rotating channel flow. (a) Mean velocity, (b) turbulent shear stress normalized by u_*^2, (c) turbulent kinetic energy normalized by u_*^2.

The function F in (30) can be taken as

$$F = 1.0 \tag{34}$$

which corresponds to the original eddy-viscosity coefficient (Durbin 1991) or

$$F = \frac{1+\alpha_2|\eta_3|+\alpha_3\eta_3}{1+\alpha_4|\eta_3|}\left(\sqrt{\frac{1+\alpha_5\eta_1}{1+\alpha_5\eta_2}}+\alpha_1\sqrt{\eta_2}\sqrt{|\eta_3|-\eta_3}\right)^{-1} \tag{35}$$

which is the modification proposed by Pettersson Reif *et al.* (1999) in order to account for rotational effects. Model coefficients are given by

$$C_\mu = 0.21, C_\omega = 2.25 \tag{36}$$

$$\alpha_1 = 0.055\sqrt{f_1} = 0.275\alpha_4, \alpha_2 = \frac{1}{2}f_1 = 2\alpha_3, \alpha_5 = \frac{1}{40}, f_1 = 1.65\sqrt{\frac{\overline{v^2}}{k}} \tag{37}$$

The dimensionless velocity gradient parameters are given by

$$\eta_1 = \tau^2|S^2|, \eta_2 = \tau^2|W^{*2}|, \eta_3 = \eta_1 - \eta_2. \tag{38}$$

In the following subsections, the proposed constitutive relationship (29) is used in conjunction with the $\overline{v^2}-f$ model. The modified $C^*_{\mu 1}$ coefficient (35) has been used in all computations presented herein.

2.3.1 Homogeneous shear flow

Consider homogeneous shear flow where

$$\mathrm{S} = \begin{pmatrix} 0 & \frac{1}{2}S & 0 \\ \frac{1}{2}S & 0 & 0 \\ 0 & 0 & 0 \end{pmatrix} \tag{39}$$

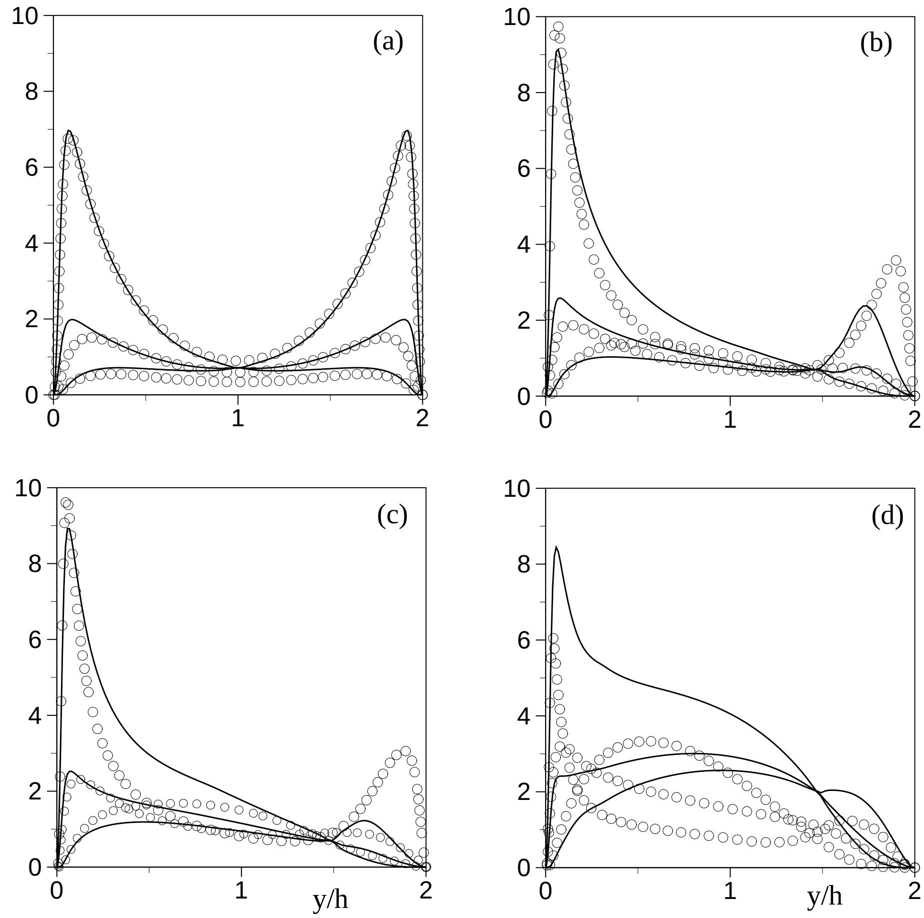

FIGURE 2. Rotating channel flow. Reynolds normal stresses normalized by u_*^2. (a) Ro = 0.0, (b) Ro = 0.1, (c) Ro=0.2, (d) Ro=0.5. Symbols: DNS. LInes: Present.

$$\mathrm{W}^* = \begin{pmatrix} 0 & \frac{1}{2}S & 0 \\ -\frac{1}{2}S & 0 & 0 \\ 0 & 0 & 0 \end{pmatrix} \tag{40}$$

The components of the anisotropy tensor $b_{ij} = \overline{u_i u_j}/2k - \delta_{ij}/3$ are given by

$$b_{12} = -C_{\mu 1}^{*\infty} \left(\frac{\overline{v^2}}{k} \right)_\infty \left(\frac{Sk}{\varepsilon} \right)_\infty = -0.185 \tag{41}$$

$$b_{11} = \left(\frac{1}{4} C_{\mu 2}^{*\infty} + \frac{1}{24} C_{\mu 3}^{*\infty} \right) \left(\frac{2}{3} - \frac{\overline{v^2}}{k} \right)_\infty \left(\frac{Sk}{\varepsilon} \right)_\infty^2 = 0.197 \tag{42}$$

$$b_{22} = \left(-\frac{1}{4} C_{\mu 2}^{*\infty} + \frac{1}{24} C_{\mu 3}^{*\infty} \right) \left(\frac{2}{3} - \frac{\overline{v^2}}{k} \right)_\infty \left(\frac{Sk}{\varepsilon} \right)_\infty^2 = -0.137 \tag{43}$$

$$b_{33} = -\left(b_{11} + b_{22} \right) = -0.060$$

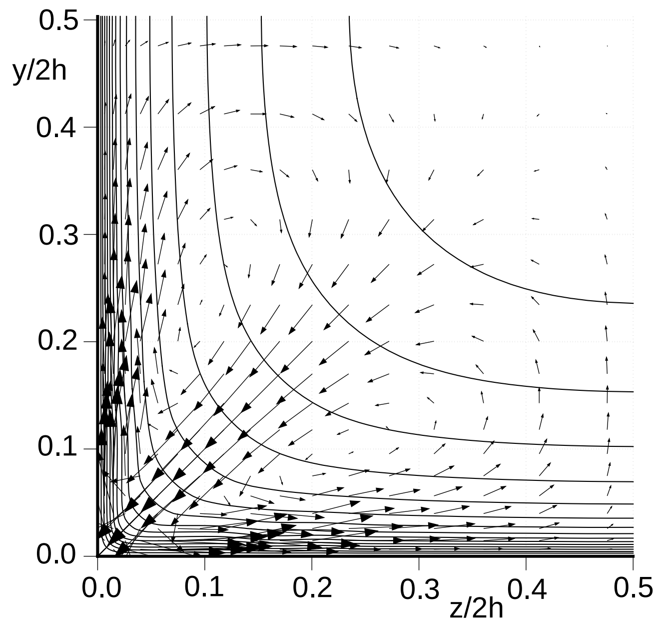

FIGURE 3. Square duct flow. Vectors: secondary mean flow field; Contours: mean streamwise velocity. Results plotted in one quadrant of the duct.

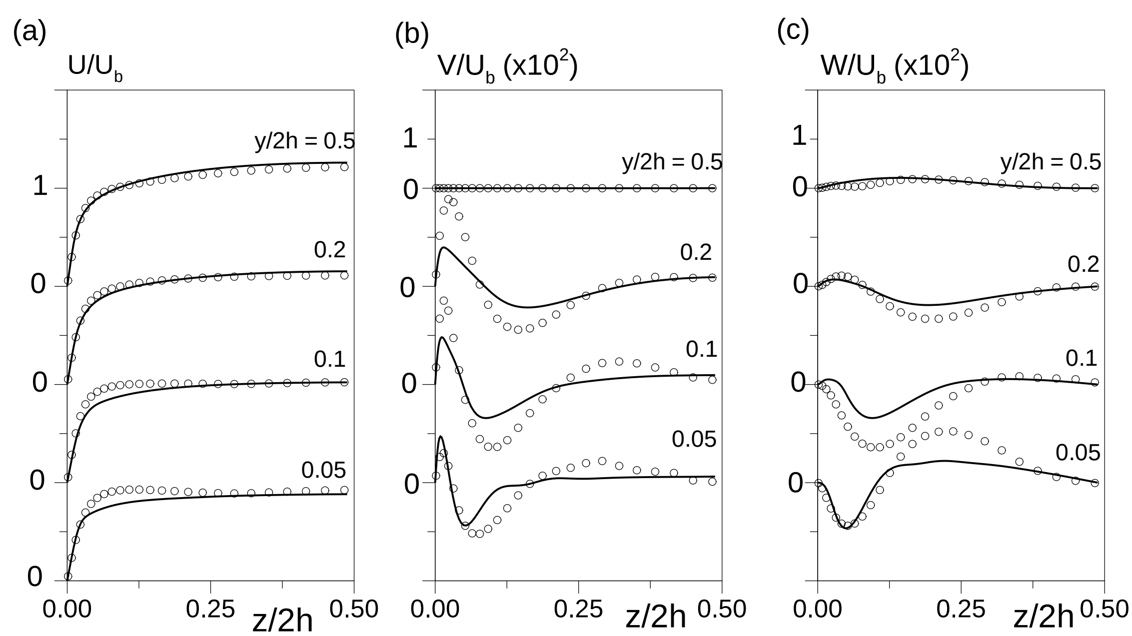

FIGURE 4. Square duct flow. Mean velocity field: (a) primary component, (b) and (c) secondary components. Symbols: DNS; Lines: predictions.

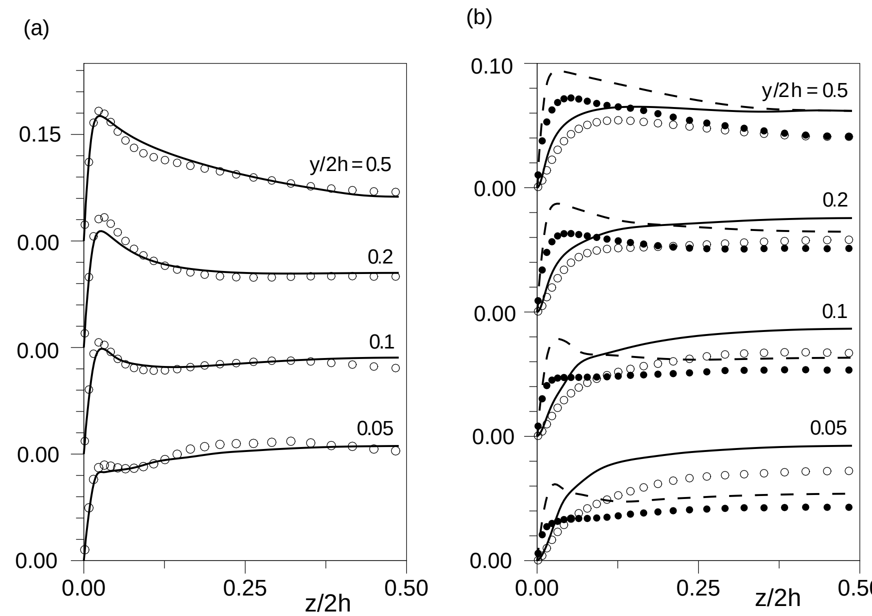

FIGURE 5. Square duct flow. Reynolds normal stresses: (a) Streamwise component $\sqrt{u^2}/U_b$ (b) Cross-stream components $\sqrt{v^2}/U_b$ (——— , open symbols) and $\sqrt{w^2}/U_b$ (– – – – , filled symbols). Symbols: DNS; Lines: predictions.

Here, the equilibrium values $\left(\overline{v^2}/k\right)_\infty = 0.367$, $(Sk/\varepsilon)_\infty = 4.807$ and $C_{\mu1}^{*\infty} = 0.21$ have been used. The results corresponds reasonable well with the experimental data of Tavoularis & Corrsin (1981); $(b_{11}, b_{22}, b_{33}) = (0.202, -0.145, -0.057)$. The SSG model gives $(b_{11}, b_{22}, b_{33}) = (0.205, -0.150, -0.055)$.

2.3.2 Rotating channel flow

Fully developed unidirectional channel flow subjected to orthogonal mode rotation was considered by Pettersson Reif *et al.* (1999) to assess the performance of the strain-dependent eddy-viscosity coefficient $C_{\mu1}^*$. The response of system rotation enters only through the linear term in this particular case. The anisotropy of the Reynolds-stresses does not influence on the turbulent shear stress and, henceforth, not on the mean velocity or turbulent kinetic energy either. Figure 1 displays the predicted mean velocity, turbulent shear stress, and kinetic energy, respectively, at $Re_* \equiv hu_*/\nu = 194$ and different $Ro \equiv 2h\Omega/U_b$ (Pettersson Reif *et al.* 1999). Here U_b and $2h$ denote the mean bulk velocity and channel height respectively. The predictions are compared with the DNS data reported by Kristoffersen & Andersson (1993).

Figure 2 displays the predicted normal stresses. The new model returns anisotropies in close agreement with the DNS data. Recall that the linear model predicts $\overline{u_\alpha^2} = \frac{2}{3}k$.

2.3.3 Square duct flow

Fully developed flow inside a straight square duct constitutes another frequently used test case for the assessment of closure models. The main characteristic of this flow is the occurrence of a secondary flow field in the plane perpendicular to the primary flow direction. This secondary mean flow field is generated by the turbulence, in particular by the anisotropy of the turbulence field. Linear eddy-viscosity models can therefore not predict this phenomenon.

The predicted secondary flow field in Fig. 3 shows the characteristic contrarotating pair of streamwise vortices in the corner of the duct. The predominant effect of this secondary motion is the induced transfer of streamwise momentum towards the corner; the isolevels of the streamwise mean velocity becomes distorted. Figure 4 shows a detailed comparison of the predicted mean velocity field and DNS data (Huser & Biringen 1993) at $Re_* \equiv 2hu_*/\nu = 600$ where $2h$ is the duct height and u_* is the averaged wall friction velocity.

Figure 5 displays the distribution of Reynolds normal stresses. The model predictions are in reasonable agreement with the DNS data although the turbulent kinetic energy is somewhat overpredicted.

2.4 Future plans

The premise of this study was that the predictive capability of the $\overline{v^2} - f$ model can be increased by accounting for turbulent anisotropies. This require a nonlinear constitutive relationship which constitutes a major change of the otherwise successful linear model. The new model should not return results that are significantly different from the original linear model in cases where the latter performs well. In other cases, the quality of the predictions should improve. The new model needs, therefore, to be further tested in a wide variety of flows of engineering interest.

REFERENCES

DURBIN, P. A. 1991 Near-wall turbulence closure modeling without 'damping functions'. *Theor. Comp. Fluid Dyn.* **3,** 1-13.

DURBIN, P. A. 1995 Constitutive equation for the $k-\varepsilon-\overline{v^2}$ model. *6th Int. Symp. Comput. Fluid Dyn.* Lake Tahoe, CA, USA.

HUSER, A. & BIRINGEN, S. 1993 Direct numerical simulation of turbulent flow in a square duct. *J. Fluid Mech.* **257,** 65-95.

KRISTOFFERSEN, R. & ANDERSSON, H. I. 1993 Direct simulations of low-Reynolds-number turbulent flow in a rotating channel. *J. Fluid Mech.* **256,** 63-197.

PETTERSSON REIF, B. A., DURBIN, P. A.& OOI, A. 1999 Modeling rotational effects in eddy-viscosity closures. *Int. J. Heat & Fluid Flow* (in print).

POPE, S. B. 1975 A more general eddy-viscosity hypothesis. *J. Fluid Mech.* **72,** 331-340.

TAVOLARIS, S. & CORRSIN, S. 1981 Experiments in nearly homogeneous turbulent shear flows with a uniform mean temperature gradient. *J. Fluid Mech.* **104,** 311-347.